International Journal of Nanomedicine

Dovepress
open access to scientific and medical research

Open Access Full Text Article

ORIGINAL RESEARCH

Synthesis, characterization, and efficacy of antimicrobial chlorhexidine hexametaphosphate nanoparticles for applications in biomedical materials and consumer products

International Journal of Nanomedicine downloaded from https://www.dovepress.com/
For personal use only.

This article was published in the following Dove Press journal:
International Journal of Nanomedicine
18 August 2013
Number of times this article has been viewed

Michele E Barbour[1]
Sarah E Maddocks[2]
Natalie J Wood[1,3]
Andrew M Collins[3]

[1]Oral Nanoscience, School of Oral and Dental Sciences, University of Bristol, Bristol, UK; [2]Cardiff School of Health Sciences, Cardiff Metropolitan University, Cardiff, UK; [3]Bristol Centre for Functional Nanomaterials, University of Bristol, Bristol, UK

Abstract: Chlorhexidine (CHX) is an antimicrobial agent that is efficacious against gram-negative and -positive bacteria and yeasts. Its mechanism of action is based on cell membrane disruption and, as such, it does not promote the development of bacterial resistance, which is associated with the widespread use of antibiotics. In this manuscript, we report the development of novel antimicrobial nanoparticles (NPs) based on a hexametaphosphate salt of CHX. These are synthesized by instantaneous reaction between equimolar aqueous solutions of CHX digluconate and sodium hexametaphosphate, under room temperature and pressure. The reaction results in a stable colloid composed of highly negatively charged NPs (−50 mV), of size 20–160 nm. The NPs adhere rapidly to specimens of glass, titanium, and an elastomeric wound dressing, in a dose-dependent manner. The functionalized materials exhibit a gradual leaching of soluble CHX over a period of at least 50 days. The NP colloid is efficacious against methicillin-resistant *Staphylococcus aureus* (MRSA) and *Pseudomonas aeruginosa* in both planktonic and biofilm conditions. These NPs may find application in a range of biomedical and consumer materials.

Keywords: MRSA, biomaterials, chlorhexidine, drug delivery, slow release

Introduction

Chlorhexidine (CHX) is a broad spectrum antimicrobial in widespread use in medical care. It is used in preoperative skin cleansing preparations, hand disinfectants, and oral mouth rinses. It is efficacious against gram-positive and -negative bacteria and many yeast species. Its mechanism of action is related to its crossing the cell envelope and inducing the leakage of intracellular constituents; this is a rapid process, with most damage occurring within 20 seconds of exposure.[1]

The threat of the microbial evolution of antibiotic resistance is accepted to be of acute concern to the global community. For this reason there is a strong impetus to develop antimicrobial strategies that do not encourage the evolution of such resistance. The possibility of microbial resistance to CHX has been investigated extensively and it has become apparent that, while individual populations of microbes can become less sensitive to CHX when subjected to increasing environmental concentrations, this is reversed when the CHX stimulus is removed, indicating that such changes are reversible and do not represent a true resistance.[2] For this reason, CHX has been described as a good candidate for the development of materials and devices with antimicrobial properties that do not add to the burden on antibiotics.[3]

Correspondence: Michele E Barbour
School of Oral and Dental Sciences,
Lower Maudlin St, Bristol BS1 2LY, UK
Tel +44 117 342 4419
Email m.e.barbour@bristol.ac.uk

© 2013 Barbour et al. This work is published by Dove Medical Press Ltd, and licensed under Creative Commons Attribution – Non Commercial (unported, v3.0) License. The full terms of the License are available at http://creativecommons.org/licenses/by-nc/3.0/. Non-commercial uses of the work are permitted without any further permission from Dove Medical Press Limited, provided the work is properly attributed. Permissions beyond the scope of the License are administered by Dove Medical Press Limited. Information on how to request permission may be found at: http://www.dovepress.com/permissions.php

CHX is most commonly used in the form of CHX digluconate, a readily soluble salt, in aqueous solution. Some biomedical materials have been rendered temporarily antimicrobial by soaking in CHX digluconate solutions.[4,5] It is also sometimes used in the form of CHX diacetate, and this has been added as a dry crystalline powder to a number of materials with the intention of conferring antimicrobial properties on them.[6–8] In this manuscript, we report the synthesis and characterization of novel CHX-based nanoparticles (NPs) that exhibit a long-term release of soluble CHX and go on to explore their CHX elution profiles, distribution, and structure on medically relevant materials, and their antimicrobial efficacy.

Materials and methods

Synthesis and characterization of nanoparticles

Chlorhexidine hexametaphosphate (CHX-HMP) NPs were prepared by combining, at room temperature and pressure and under rapid stirring, CHX (as the digluconate salt in aqueous solution) and hexametaphosphate (HMP) (as the sodium salt in aqueous solution) (both supplied by Sigma Aldrich Corp, St Louis, MO, USA) to effect final total concentrations of 5 and 0.5 mmol L^{-1}, respectively, of each. The resultant nanoparticulate salts are referred to as CHX-HMP-5 and CHX-HMP-0.5, respectively.

Mixing the two reagents resulted in the instantaneous formation of a colloidal suspension. The particle size and zeta potential of the NPs in the colloidal suspensions were characterized using dynamic light scattering (DLS) (Malvern Zetasizer Nano-ZS, Malvern Instruments Ltd, Malvern, UK) as a function of time.

Preparation and characterization of nanoparticle-functionalized materials

Specimens of three materials were coated with the NPs (Table 1). An amount of 200 mL of the colloidal suspension was prepared using freshly-prepared reagents (to prevent hydrolysis of the HMP). Each specimen was immersed in the rapidly stirred colloid for 30 seconds, then removed and immersed in deionized water for 10 seconds to rinse, and then, blotted to remove excess liquid and allowed to dry in air.

Nanoparticle-functionalized titanium (Grade 2 commercially pure titanium sheet, 1mm thickness; Ti-TEK Ltd, Sutton Coldfield, UK) and glass (AGF7011; Agar Scientific, Stansted, UK) surfaces were examined using atomic force microscopy (AFM) (NanoScope® IIIa, Veeco, Plainview, NY, USA). The glass coverslips were suitably flat for AFM analysis, without modification. The alginate fiber wound dressings (Savlon® Alginate Dressings; Novartis Pharmaceuticals Corp, Basel, Switzerland) were too rough to be amenable to AFM imaging. The polished titanium was also unacceptably rough in comparison with the size of the NPs, and thus for microscopy analysis, flatter titanium specimens were prepared by vacuum-coating titanium onto glass coverslips. The coverslips were cleaned with Balzer Substrate cleaner, No 1 and No 2 (Pfeiffer Vacuum GmbH, Asslar, Germany), and then loaded in calotte plates (Balzer AG, Balzers, Liechstenstein) so that they could be mounted in a Balzer TPH 510 Vacuum Coater (Pfeiffer Vacuum GmbH), with the surfaces to be coated facing downwards. The system was evacuated to a base pressure of 5×10^{-5} Torr and, after 1 hour, a flow of air was introduced using a needle valve to raise the chamber pressure to 50 mTorr. A glow discharge plasma of 150 W was generated at this pressure and maintained for 10 minutes to prepare the sample surfaces for metal coating. After plasma treatment, the needle valve was closed, and the chamber was baked at 130°C for 8 hours to lower the pressure to 2×10^{-6} Torr. The titanium was flash-evaporated from tungsten boats at a rate of 1000 Hz s^{-1} to deposit a metal film 100 nm (2100 Hz) thick on the samples. During evaporation, the calotte plate holder was rotated at 100 rpm to ensure the metal film was of optimal uniformity.

The nanofunctionalized titanium, glass, and alginate fiber wound dressing specimens were examined using a scanning

Table 1 Materials functionalized with antimicrobial nanoparticles

Shorthand name	Description	Preparation	Supplier
Glass	12 mm diameter circular borosilicate glass cover slips	10-minute ultrasonication in acetone, 10-minute ultrasonication in industrial methylated spirits, air dry	Agar Scientific, Stansted, UK
Alginate wound dressing	10 × 7 mm sections of a commercially available wound dressing containing alginate fibers	Used as supplied	Savlon® Alginate Dressings, Novartis Pharmaceuticals Corp, Basel, Switzerland
Titanium	10 × 10 × 1 mm square sections of grade 2, commercially pure titanium	Polished using 80 grit silicon carbide paper, 10-minute ultrasonication in acetone, 10-minute ultrasonication in industrial methylated spirits, air dry	Ti-TEK Ltd, Sutton Coldfield, UK

electron microscopy (SEM) (Phenom, Phenom-World, Eindhoven, Netherlands) after coating with gold-palladium alloy, using a sputter coating unit (SC7620, Quorum Technologies, East Grinstead, UK). Since neither glass nor titanium were atomically flat surfaces, it was difficult to distinguish between small (<20 nm) surface features and small NPs; for this reason, the CHX-HMP-5 and CHX-HMP-0.5 NPs were also deposited on freshly cleaved mica (AGF7013, Agar Scientific) and subjected to AFM to resolve the smallest among them.

CHX elution from nanoparticle-functionalized materials

Eight specimens of each material coated with the CHX-HMP-5 and CHX-HMP-0.5 NPs were placed in individually labeled cuvettes suitable for ultraviolet spectrophotometry. Deionized water was added to the cuvettes, and they were sealed tightly using cuvette lids. These were agitated on an orbital shaker rotating at 150 rpm (Stuart® SSM1; Bibby Scientific Ltd, Stone, UK). The cuvettes were kept sealed and were sampled for CHX concentration at intervals over a 60-day period, by measuring absorbance at 255 nm and comparing the readings to calibration standards of 5–50 μmol L^{-1} CHX.[9] Control sets were prepared, where the specimens were immersed in deionized water and where they were immersed in a 25 μmol L^{-1} CHX solution, which was the residual concentration of aqueous CHX in the CHX-HMP-5 colloidal suspension.

Microbiology

Bacterial strains

Methicillin-resistant *Staphylococcus aureus* (MRSA) (NCTC 13142; Public Health England, Salisbury, UK) was cultured in Mueller-Hinton (MH) media (Sigma Aldrich). *Pseudomonas aeruginosa* NCIMB 8626 (ATCC 9027; American Type Culture Collection, Manassas, VA, USA) was cultured in nutrient broth (NB) or nutrient agar (NA) (N7519 or N9405; Sigma Aldrich). All cultures were incubated at 37°C under aerobic conditions throughout the study.

Minimum inhibitory concentrations

The minimum inhibitory concentration (MIC) for the control aqueous 25 μM CHX and the CHX-HMP-5 colloid against planktonic bacteria was determined by serial doubling the dilution (0–25 μmol L^{-1}) in a total volume of 100 μL of appropriate media (MH media for MRSA, NB for *P. aeruginosa*) in a 96-well microtiter plate (according to British Society for Antimicrobial Chemotherapy methodology for determining MIC[10]). The cultures were incubated for 16 hours at 37°C in aerobic conditions, and optical density (OD) readings were measured at 620 nm (A_{620}) using a standard microtiter plate reader (SPECTROstar Nano; BMG Labtech GmbH, Ortenburg, Germany).

Total viable counts

The samples were taken from the wells of the microtiter plate and serially diluted (10^{-1}–10^{-6}) in phosphate buffered saline (PBS) (Sigma Aldrich); 10 μL aliquots were enumerated using the total viable cell counting method of Miles and Misra,[11] with MH or NA as a nonselective medium. The numbers of recovered cells were calculated as colony forming units per mL (cfu mL^{-1}).

Static biofilm model

The bacterial strains were initially grown for 16 hours, and these stationary phase cultures were harvested by centrifugation, and adjusted to OD_{650} = 0.1. Biofilms were aerobically grown in 50 μL of appropriate media (MH media for MRSA, NB for *P. aeruginosa*) at 37°C for 48 hours; then, the media was removed and discarded. Loosely adherent bacteria were removed by washing the biofilms twice with 100 μL PBS. CHX or CHX NPs, diluted in PBS, were added to the biofilms using a doubling dilution, as described above (0–25 μmol L^{-1}). The plates were incubated for 2 hours at 37°C; to estimate the biomass, unattached cells were gently aspirated and discarded, and adherent cells were washed twice with PBS and stained with crystal violet (0.25% w v^{-1}) (Sigma Aldrich) for 10 minutes; following a further two washes with PBS, the cell-bound crystal violet was resolubilized with 7% acetic acid (Sigma Aldrich), and absorbance measured at 595 nm (A_{595}).

Results

The mean particle size, as measured by DLS, and the zeta potential of the CHX-HMP-0.5 and CHX-HMP-5 suspensions are shown in Table 2. It is possible that smaller particles were also present in the colloid, since in DLS,

Table 2 Particle size and zeta potential of CHX-HMP-0.5 and CHX-HMP-5 preparations measured using DLS and electrophoretic mobility measurements

Nanoparticle preparation	Particle size [nm] (SD)	Zeta potential [mV] (SD)
CHX-HMP-0.5	81 (13)	–45 (2)
CHX-HMP-5	157 (7)	–50 (3)

Notes: This shows the dominant particle size as having the strongest signal. The signal is proportional to (diameter)6 and thus, it is likely that this represents the upper limit of the nanoparticle size. In some cases, a bimodal signal distribution indicated the presence of nanoparticles with diameters as low as 20–60 nm.
Abbreviations: CHX-HMP-0.5, chlorhexidine hexametaphosphate (0.5 mmol L^{-1}); CHX-HMP-5, chlorhexidine hexametaphosphate (5 mmol L^{-1}); DLS, dynamic light scattering; SD, standard deviation.

the signal is proportional to particle diameter to the sixth power, and thus the signal will be very much dominated by the largest population. The microscopy results would also support smaller particles mixed in with the larger ones. The SEM images of the NP-functionalized alginate fiber wound dressing, glass, and titanium surfaces are shown in Figures 1–3, and the AFM of the NP-functionalized glass, titanium, and mica surfaces are shown in Figures 4–6. The

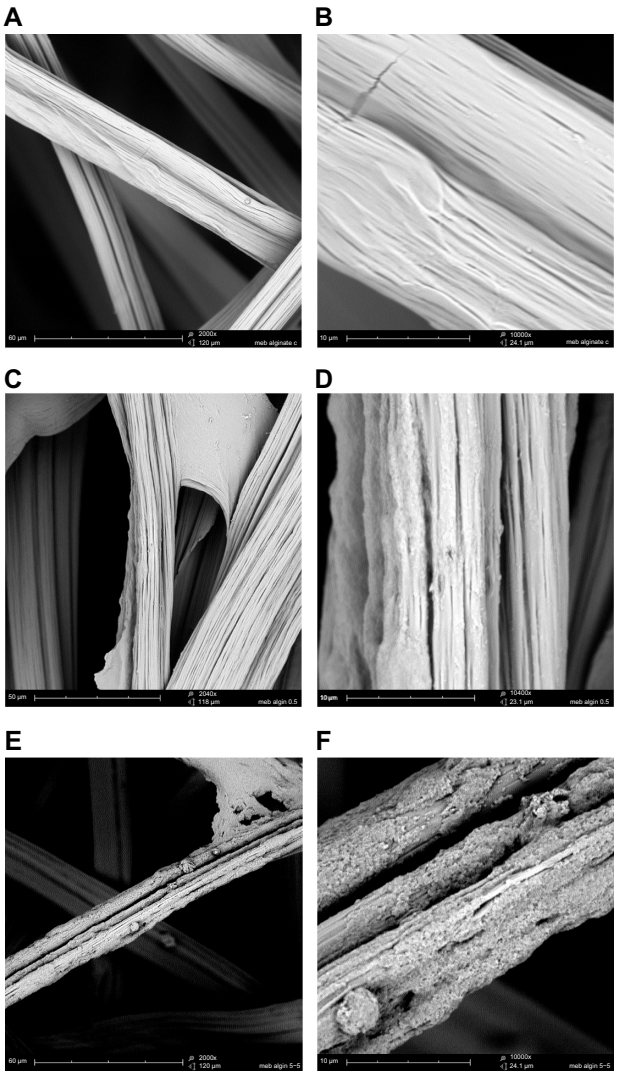

Figure 1 CHX-HMP nanoparticles on an alginate wound dressing: (**A** and **B**) control (no nanoparticles); (**C** and **D**) CHX-HMP-0.5 nanoparticles; and (**E** and **F**) CHX-HMP-5 nanoparticles.

Notes: The untreated wound dressing showed 10–25 μm diameter fibers, many of which consisted of bundles of smaller fibers, with moderately smooth surfaces (**A** and **B**). The CHX-HMP-0.5-functionalized dressing showed some areas where a precipitate could be observed on the surface of the fibers (**C** and **D**), while others appeared to be unchanged, at least, at the resolution of this microscope. The CHX-HMP-5-functionalized dressing exhibited large deposits of the porous nanoparticle aggregate seen on other specimens (**E** and **F**), and this was present on almost all fibers observed during SEM analysis. **A**, **C**, and **E** were taken at original magnification 2000x; the scale bar is 50/60 μm. **B**, **D**, and **F** were taken at original magnification 1000x; scale bar is 10 μm.

Abbreviations: CHX-HMP, chlorhexidine hexametaphosphate; CHX-HMP-0.5, chlorhexidine hexametaphosphate (0.5 mmol L^{-1}); CHX-HMP-5, chlorhexidine hexametaphosphate (5 mmol L^{-1}); SEM, scanning electron microscope.

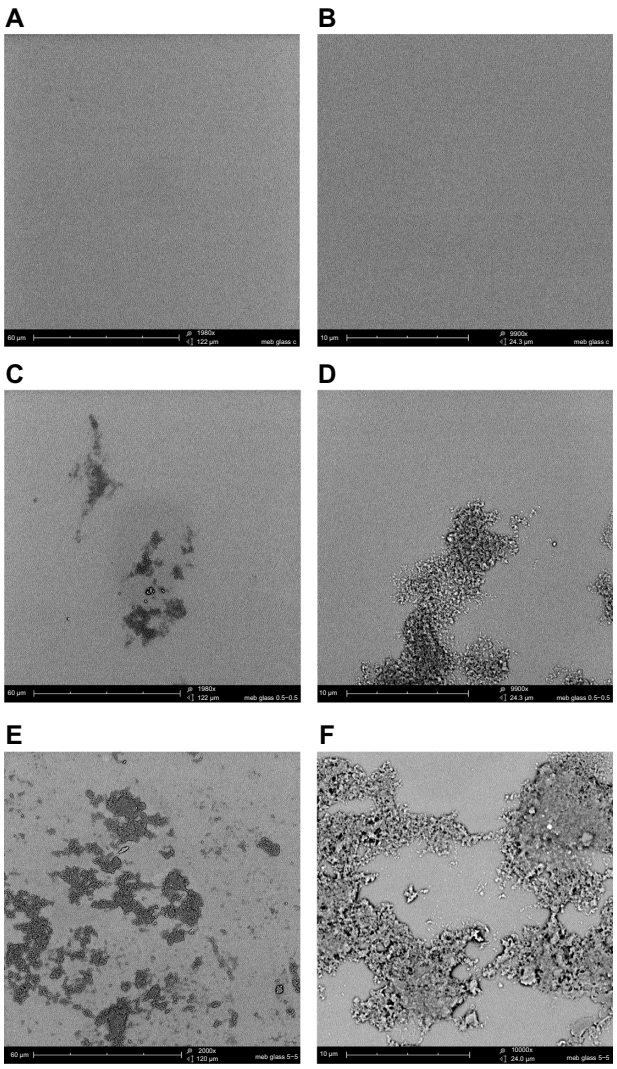

Figure 2 CHX-HMP nanoparticles on glass cover slips: (**A** and **B**) control (no nanoparticles); (**C** and **D**) CHX-HMP-0.5 nanoparticles; and (**E** and **F**) CHX-HMP-5 nanoparticles.

Notes: The untreated glass cover slip appeared smooth and featureless. The CHX-HMP-0.5 surface displayed aggregations of nanoparticles forming a self-assembled porous architecture; these were sparsely distributed. The CHX-HMP-5 surface displayed similar deposits of the porous aggregate, but these were more widespread, covering much of the surface. **A**, **C**, and **E** were taken at original magnification 2000x; the scale bar is 60 μm. **B**, **D**, and **F** were taken at original magnification 1000x; scale bar is 10 μm.

Abbreviations: CHX-HMP, chlorhexidine hexametaphosphate; CHX-HMP-0.5, chlorhexidine hexametaphosphate (0.5 mmol L^{-1}); CHX-HMP-5, chlorhexidine hexametaphosphate (5 mmol L^{-1}).

titanium and glass specimens exhibited nanoscale roughness which made it impossible to distinguish the substrate surface from NPs with diameter less than around 40 nm, but the control mica surface was atomically flat, and these images gave clear indications of a confluent layer of NPs with diameters of 20–100 nm.

The CHX elution from the NP-functionalized alginate fiber wound dressing, glass, and titanium surfaces, as a function of time, is shown in Figures 7–9. All NP-functionalized specimens exhibited soluble CHX release; the magnitude,

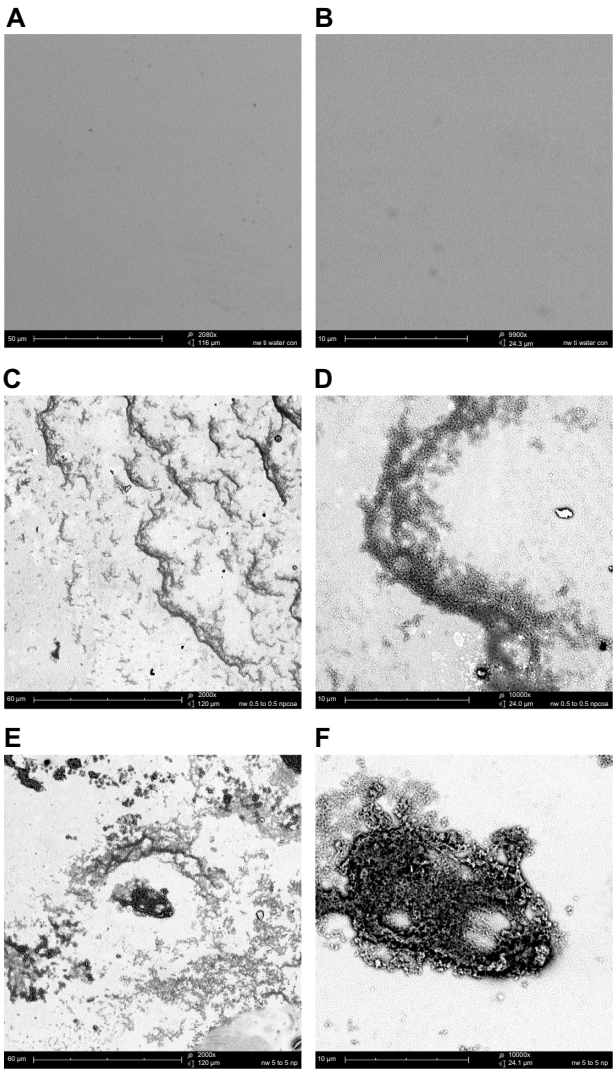

Figure 3 CHX-HMP nanoparticles on titanium: (**A** and **B**) control (no nanoparticles); (**C** and **D**) CHX-HMP-0.5 nanoparticles; and (**E** and **F**) CHX-HMP-5 nanoparticles.
Notes: The untreated titanium appeared featureless at this resolution. The CHX-HMP-0.5 surface was coated with small deposits of the nanoparticles. The CHX-HMP-5 surface displayed larger aggregates of the nanoparticles across much of the surface. **A**, **C**, and **E** were taken at original magnification 2000x; the scale bar is 50/60 μm. **B**, **D**, and **F** were taken at original magnification 1000x; scale bar is 10 μm.
Abbreviations: CHX-HMP, chlorhexidine hexametaphosphate; CHX-HMP-0.5, chlorhexidine hexametaphosphate (0.5 mmol L^{-1}); CHX-HMP-5, chlorhexidine hexametaphosphate (5 mmol L^{-1}).

dose response, and time dependence of this varied with specimen type.

The MIC for MRSA for the CHX-HMP-5 colloidal suspension equated to an 8× dilution of the colloid, which corresponded to a total (soluble and bound) CHX concentration of 0.625 mmol L^{-1} and a soluble CHX concentration of 3.12 μmol L^{-1}. The MIC for MRSA could not be established for 25 μmol L^{-1} CHX, indicating that this solution was not effectively inhibitory against MRSA. For *P. aeruginosa*, the MIC for CHX-HMP-5 equated to a 16× dilution of the colloid, which was the minimum concentration tested; this corresponded to a total CHX concentration of 0.312 mmol L^{-1} and a soluble CHX concentration of 1.56 μmol L^{-1}. The MIC for the 25 μmol L^{-1} CHX concentration was the undiluted solution, ie, 25 μmol L^{-1}, indicating that *P. aeruginosa* was more susceptible than MRSA to the NPs. The total viable cell count confirmed the MIC data, with 1.5×10^{13} cfu mL^{-1} recovered for the MRSA untreated control and no bacteria recovered from samples grown with 8× and 4× dilutions of the CHX-HMP-5 colloid, suggesting that the MIC was also bactericidal. Similarly, for *P. aeruginosa*, no bacteria could be recovered from samples grown at 16× and 8× dilution of the CHX-HMP-5 colloid, compared with 1.34×10^{9} cfu mL^{-1} recovered for the untreated control.

Biofilms of MRSA were disrupted by the CHX-HMP-5 colloid and to a lesser extent by the aqueous 25 μmol L^{-1} CHX (Figure 10). The CHX-HMP-5 colloid also disrupted the biofilms of *P. aeruginosa* more effectively than did the aqueous 25 μmol L^{-1} CHX at dilutions of between 16× and 4×; at 2× and undiluted levels, 25 μmol L^{-1} CHX and the NPs were equally effective. Neither treatment resulted in complete the removal of the biofilm for either microorganism tested (Figure 11).

Discussion

The mixing of solutions of CHX and HMP under the conditions described in this manuscript resulted in the instantaneous formation of a colloid consisting of particles of maximum average diameter 80 (CHX-HMP-0.5) and 150 (CHX-HMP-5) nm and an average zeta potential of −45 to −50 mV. The AFM and SEM images indicated individual NPs and porous NP aggregates on most surfaces exposed to the colloids. The AFM images also showed typical particle sizes of 20–160 nm. The charge of the particles resulted in a good colloidal stability, presumably owing, at least in part, to the high zeta potential,[12] with only a partial and slow sedimentation behavior demonstrated in the more concentrated preparation. The charge is also thought to be the mechanism by which the NPs adhered to the material surfaces during dip coating. The different material specimens investigated were successfully functionalized with the CHX-HMP antimicrobial NPs, and all materials exhibited a gradual leaching of soluble CHX over a period of at least 50 days.

The highest CHX release, when normalized to the surface area, was from the alginate wound dressing (Figure 7). There was an initial burst of CHX release during the first day, followed by a steady release over the experimental period. The SEM images clearly show a dense coating of NP aggregates on almost all of the fibers coated with the CHX-HMP-5 NPs

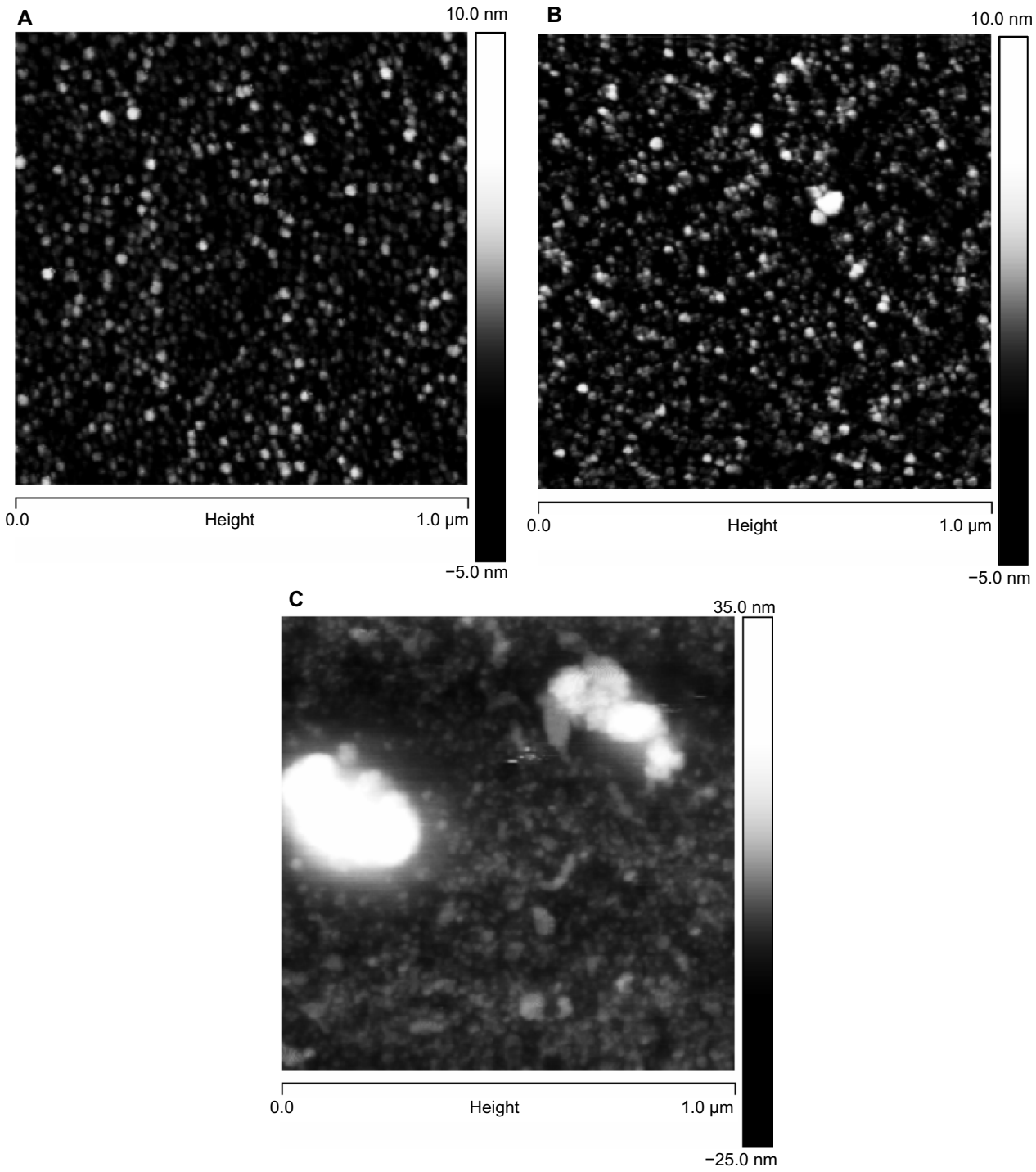

Figure 4 AFM images of glass surfaces: (**A**) untreated (cleaned) glass surface; (**B**) surface functionalized with CHX-HMP-0.5; and (**C**) surface functionalized with CHX-HMP-5.
Notes: The horizontal scale is 1 µm and the vertical scale is 15 nm (**A** and **B**) or 55 nm (**C**).
Abbreviations: AFM, atomic force microscopy; CHX-HMP-0.5, chlorhexidine hexametaphosphate (0.5 mmol L^{-1}); CHX-HMP-5, chlorhexidine hexametaphosphate (5 mmol L^{-1}).

and a sparser but readily apparent distribution on the specimens coated with CHX-HMP-0.5 NPs (Figure 1). The alginate dressing was the only specimen for which there was a significant release of CHX from the specimen treated with the control 25 µmol L^{-1} CHX solution, indicating that the material absorbed some soluble CHX from the solution, but this was considerably lower than that seen from the NP-functionalized specimens. There was a dose-response relationship whereby the CHX-HMP-5 specimens exhibited a greater release than did the CHX-HMP-0.5 specimens,

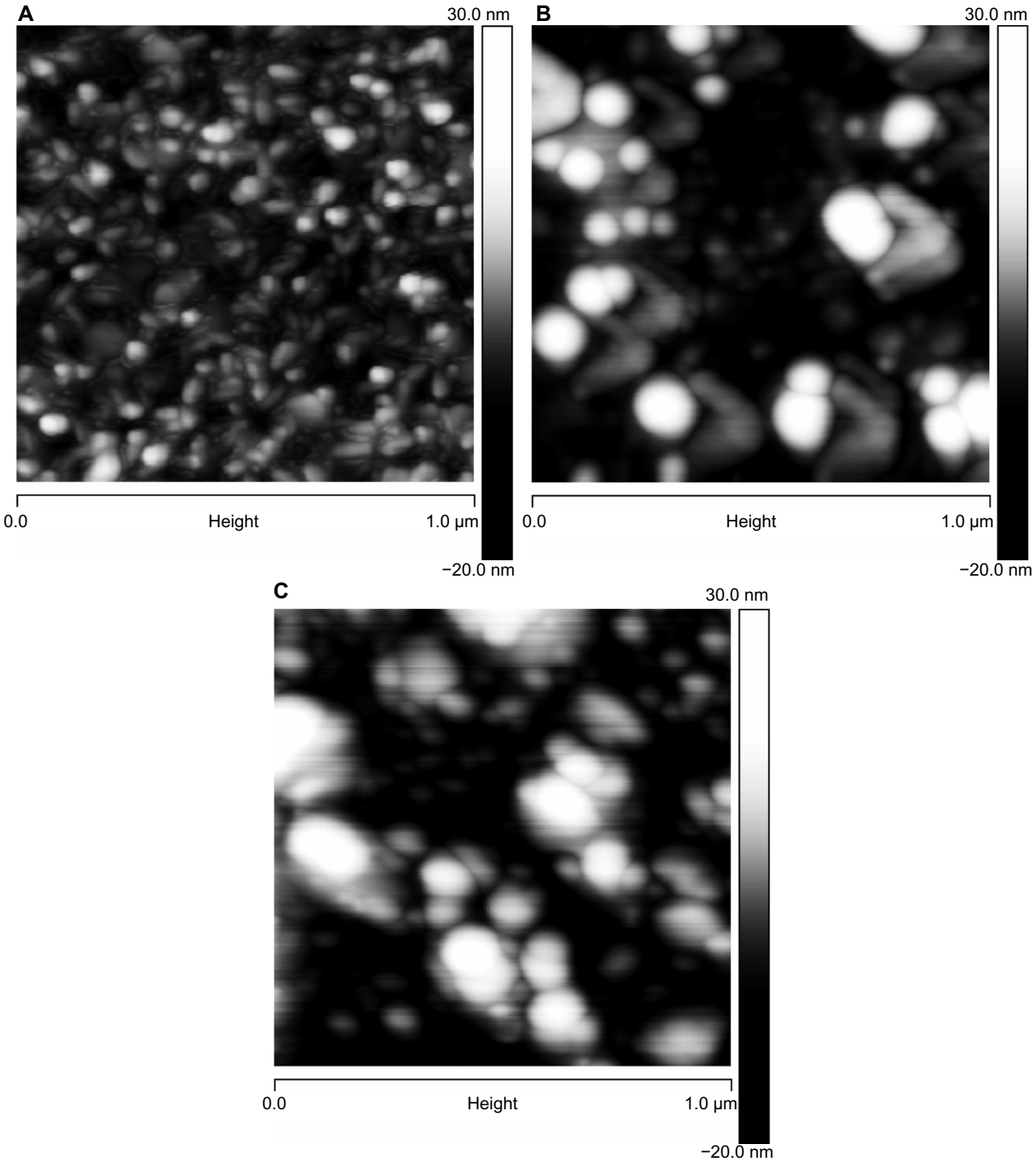

Figure 5 AFM images of titanium surfaces: (**A**) polished titanium surface; (**B**) surface functionalized with CHX-HMP-0.5; and (**C**) surface functionalized with CHX-HMP-5.
Note: The horizontal scale is 1 µm and vertical scale is 50 nm.
Abbreviations: AFM, atomic force microscopy; CHX-HMP-0.5, chlorhexidine hexametaphosphate (0.5 mmol L^{-1}); CHX-HMP-5, chlorhexidine hexametaphosphate (5 mmol L^{-1}).

and this correlated with a more widespread coverage of NPs for the CHX-HMP-5 preparation (Figure 1). For both the CHX-HMP-5 and CHX-HMP-0.5 specimens, the release was still ongoing at the conclusion of the experiment, indicating that the NPs were not depleted at this time.

These findings may be useful in developing wound dressings that protect acute and chronic or nonhealing wounds from infection. For chronic wounds, such as leg and foot ulcers, often experienced by elderly, immune-compromised, and diabetic patients, the most frequently occurring compli-

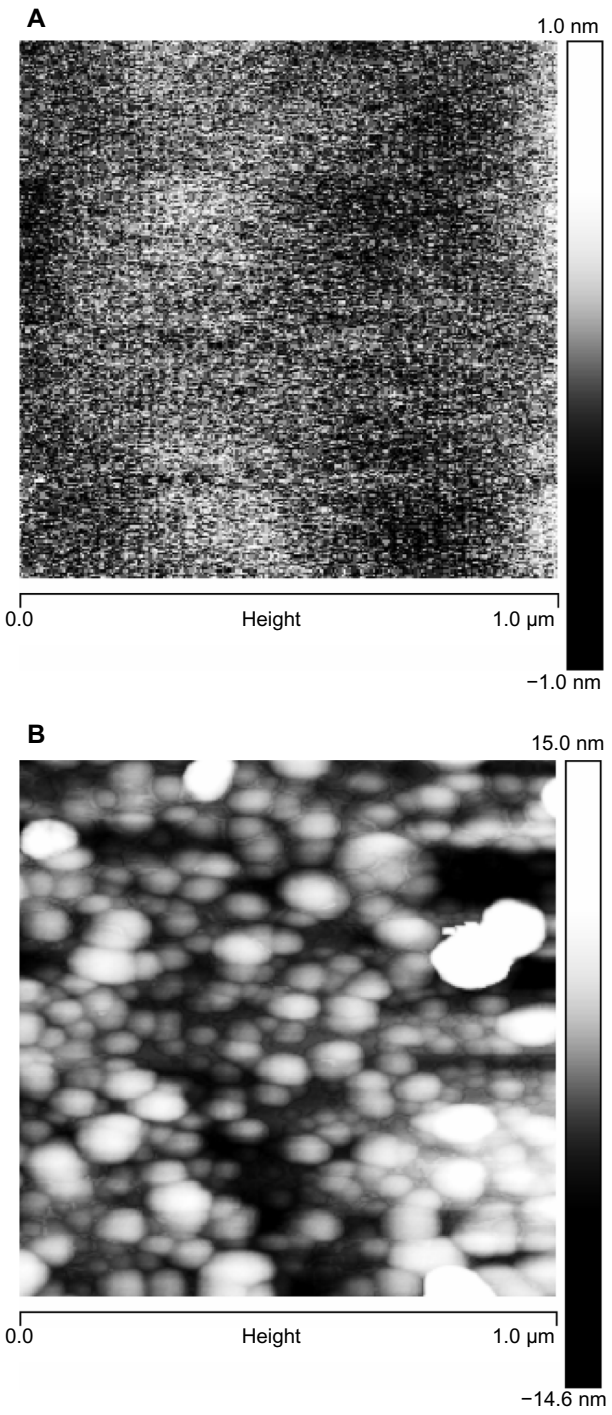

Figure 6 AFM images of mica surfaces, to show the smallest particles: (**A**) freshly cleaved mica surface, vertical scale 2 nm and (**B**) surface functionalized with CHX-HMP-0.5, vertical scale 30 nm.
Abbreviations: AFM, atomic force microscopy; CHX-HMP-0.5, chlorhexidine hexametaphosphate (0.5 mmol L^{-1}).

cation is infection.[13] Biofilms are associated with persistent or chronic wound infections.[14] There are, therefore, many studies reporting the intention to develop an antimicrobial wound dressing, and those that are efficacious against biofilms, rather than only planktonically grown bacteria, are considered to be a particular priority.[15] Some of the most common options are dressings supplemented with silver; however the clinical evidence for the use of silver-containing dressings is ambiguous at best and discouraging at worst.[16] A fibrous wound dressing that releases amoxicillin has recently been reported, although this released the bulk of its antibiotic payload within the first 2 days[17] and of course, does not address the problem of bacterial antibiotic resistance. CHX is already widely used in wound care, and CHX-soaked gauze is estimated to be one of the two most commonly used antibacterial agents in wound dressings for extremity injuries, with the other being iodine.[18] In one study, a polymer-based dressing that was soaked in an aqueous solution of CHX was shown to reduce postoperative infection in patients undergoing foot and ankle surgery.[19] Although simple soaking in CHX solution is likely to result in a rather short release of CHX, an interesting multilayered polymer wound dressing incorporating CHX diacetate has been developed, which exhibited CHX release over 8 days; longer periods were not reported.[20] The release for this dressing was measured as approximately 1 µg cm^{-2} dressing after 24 hours, which corresponds to a concentration of $(1 \times 10^4)/505 = 198$ µmol m^{-2} – very similar to the magnitude of CHX release observed from the prototype dressing reported here. After 7 days, the maximum release observed by the researchers[20] was 3 µg cm^{-2}, which corresponded to 594 µmol m^{-2}; the dressing we report took longer to release this quantity of CHX, but the release was sustained over a much longer period than that measured in the previous study. It is possible that the prolonged release of CHX may be a useful facet, particularly for dressings for nonhealing wounds. The premature removal of antimicrobial treatment often results in the recurrence of infection, as the bacterial load is reduced but not cleared; therefore, a dressing with prolonged release antimicrobial action is very attractive.

The NP-functionalized glass surfaces released CHX over the experimental period (Figure 8), and the CHX released related to the initial density of the NPs and NP aggregates, with the more densely coated CHX-HMP-5 surfaces exhibiting a higher and more prolonged release than the less densely coated CHX-HMP-0.5 surfaces (Figure 2). For the CHX-HMP-0.5 specimens, the release of soluble CHX ceased after approximately 20–25 days, whereas for the CHX-HMP-5 specimens, the release was still continuing at the 60-day point. The control group treated with 25 µmol L^{-1} CHX did not show any CHX release, indicating that the soluble CHX was fully removed by the rinsing step and therefore, that the CHX release observed with the NP-functionalized specimens was owed to the presence of these NPs. Future

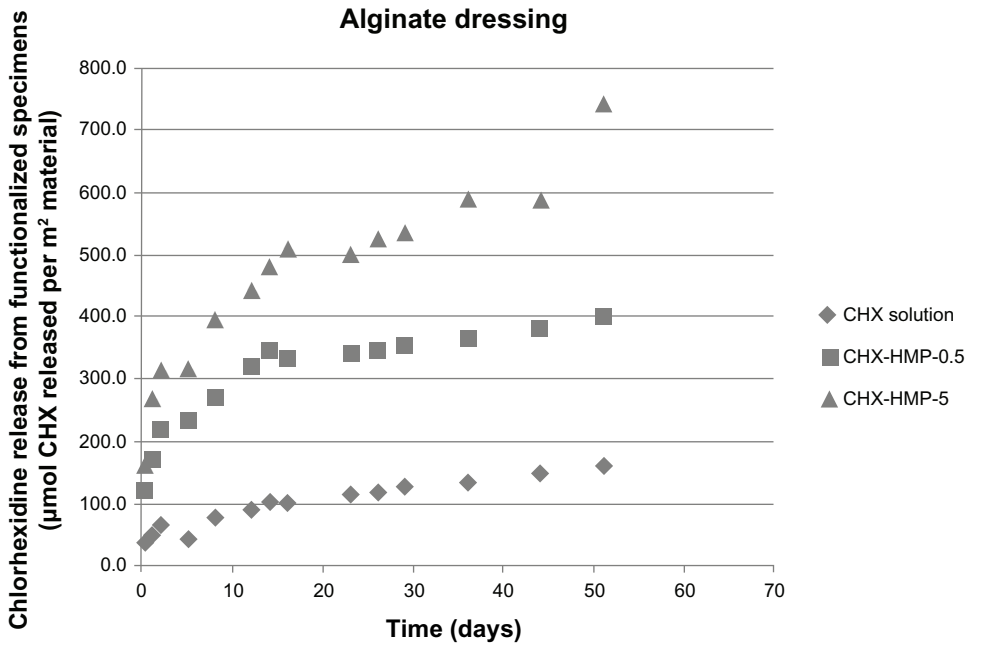

Figure 7 CHX release from nanoparticle-functionalized alginate wound dressing, expressed in μmol CHX released per unit surface area of specimen, as a function of time.

Notes: All of the wound dressings exhibited CHX release, with the highest release seen from the CHX-HMP-5-functionalized specimens and an intermediate release from the CHX-HMP-0.5 specimens. The alginate dressing was the only material that absorbed and then released CHX from the control, 25 μmol L^{-} aqueous solution of CHX. The rate of release from all nanoparticle-functionalized specimens was at its highest during the first 14–16 days and then continued at a lower rate. It was still ongoing at the conclusion of the experiment.

Abbreviations: CHX, chlorhexidine; CHX-HMP-0.5, chlorhexidine hexametaphosphate (0.5 mmol L^{-1}); CHX-HMP-5, chlorhexidine hexametaphosphate (5 mmol L^{-1}).

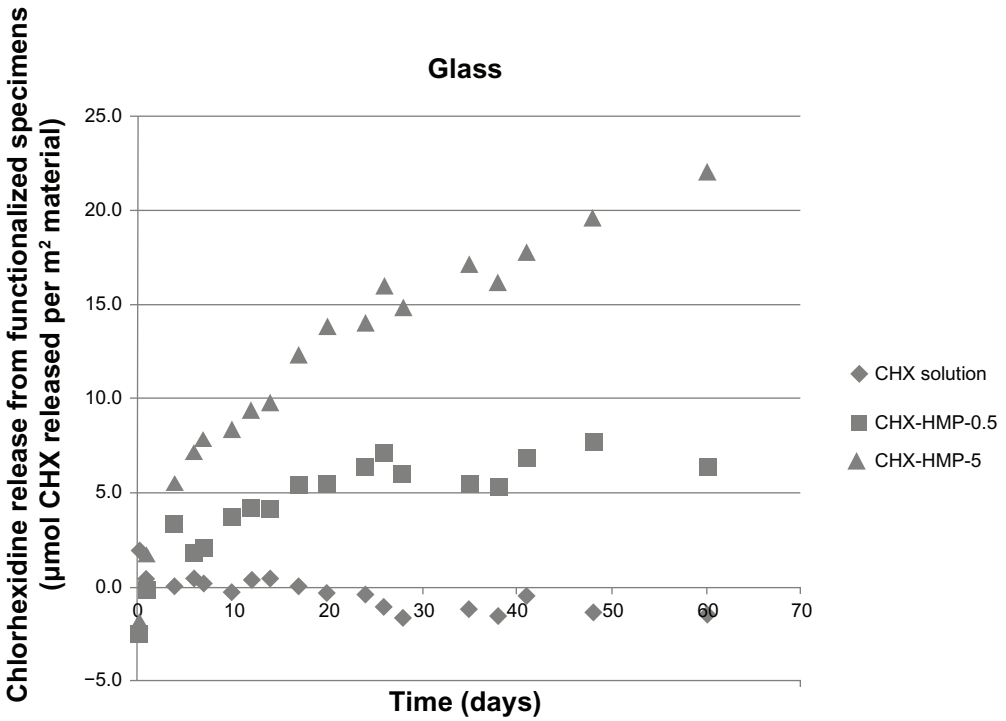

Figure 8 CHX release from nanoparticle-functionalized glass covers slips, expressed in μmol CHX released per unit surface area of specimen, as a function of time.

Notes: The CHX-HMP-5 nanoparticles showed a sustained release of soluble CHX over the 60-day measurement period, which did not appear to be approaching a plateau at the completion of the experiment. The CHX-HMP-0.5 nanoparticles showed a release that was sustained for around 20–25 days, and then, the concentration stabilized, indicating that the specimen was releasing little or no further CHX. The control specimens exposed to the aqueous solution of CHX did not show any release of CHX.

Abbreviations: CHX, chlorhexidine; CHX-HMP-0.5, chlorhexidine hexametaphosphate (0.5 mmol L^{-1}); CHX-HMP-5, chlorhexidine hexametaphosphate (5 mmol L^{-1}).

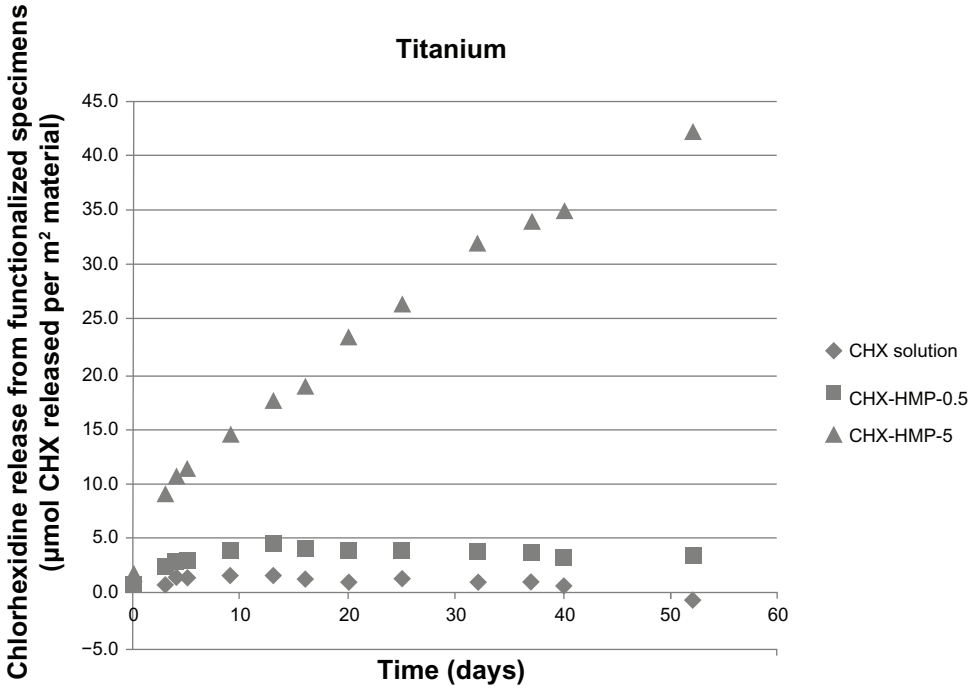

Figure 9 CHX release from nanoparticle-functionalized titanium, expressed in µmol CHX released per unit surface area of specimen, as a function of time.
Notes: The titanium functionalized with CHX-HMP-5 nanoparticles showed a sustained release of soluble CHX, which was still ongoing at the end of the experimental period. There was a lower release from the CHX-HMP-0.5 specimens; this was sustained for around 10 days, and there was little or no release after this time. The control specimens treated with 25 µmol L^{-} aqueous CHX solution did not show significant release of CHX.
Abbreviations: CHX, chlorhexidine; CHX-HMP-0.5, chlorhexidine hexametaphosphate (0.5 mmol L^{-1}); CHX-HMP-5, chlorhexidine hexametaphosphate (5 mmol L^{-1}).

studies will determine how long the NP-mediated CHX release continues and whether it can be recharged in situ.

This development may find application in glass-containing and glass-like biomedical and consumer products that would benefit from a prolonged antimicrobial functionality. One potential application is glass ionomer cement, a dental filling material that comprises fluoride-containing silica-alumina glass particles embedded in a cement matrix. Attempts to render these antimicrobial, by adding CHX digluconate or diacetate, have met with some success, although there were a few undesirable changes in mechanical properties as a result of the modifications, as well as a loss of antimicrobial efficacy over a period of a few weeks.[21] Another possible compatible material is bioglass, which finds application primarily in orthopedic implants and which has also been subject to attempts to impart antimicrobial properties, such as the infiltration of porous bioglass with silver nitrate, which resulted in a material that was efficacious against *Escherichia coli*.[22]

The titanium surfaces showed clear evidence of aggregations of the CHX-HMP NPs (Figures 3 and 5). The CHX-HMP-5-functionalized specimens showed a continuous and sustained release of soluble CHX over the duration of the experiments; numerically, this release was about double that seen from the glass surfaces. The CHX-HMP-0.5-functionalized surfaces released little CHX, and this release ceased after approximately 5 days.

The CHX-HMP-5 NPs might find application in the development of antimicrobial coatings for dental and orthopedic implants fabricated from titanium or titanium alloy. Microbial colonization of dental and orthopedic implants can have catastrophic outcomes for the patient and result in complex and costly further surgery and treatment; the development of antimicrobial coatings is therefore a very active field. For instance, the coating of titanium implants with chitosan has been achieved with the intermediate step of applying a silane coupling agent to aid retention of the coating.[23] The chemical bonding of antibiotic molecules to the implant is another approach.[24] Nanoparticulate coatings may offer an advantage over traditional antimicrobial coatings in that the NPs generate a discontinuous coating with sufficient titanium still exposed and available for colonization by osteoblast cells.

The microbiology experiments indicated that the CHX-HMP-5 colloid was efficacious against planktonically grown MRSA and *P. aeruginosa* in vitro and that this effect was not due to the residual 25 µmol L^{-1} soluble CHX present in the

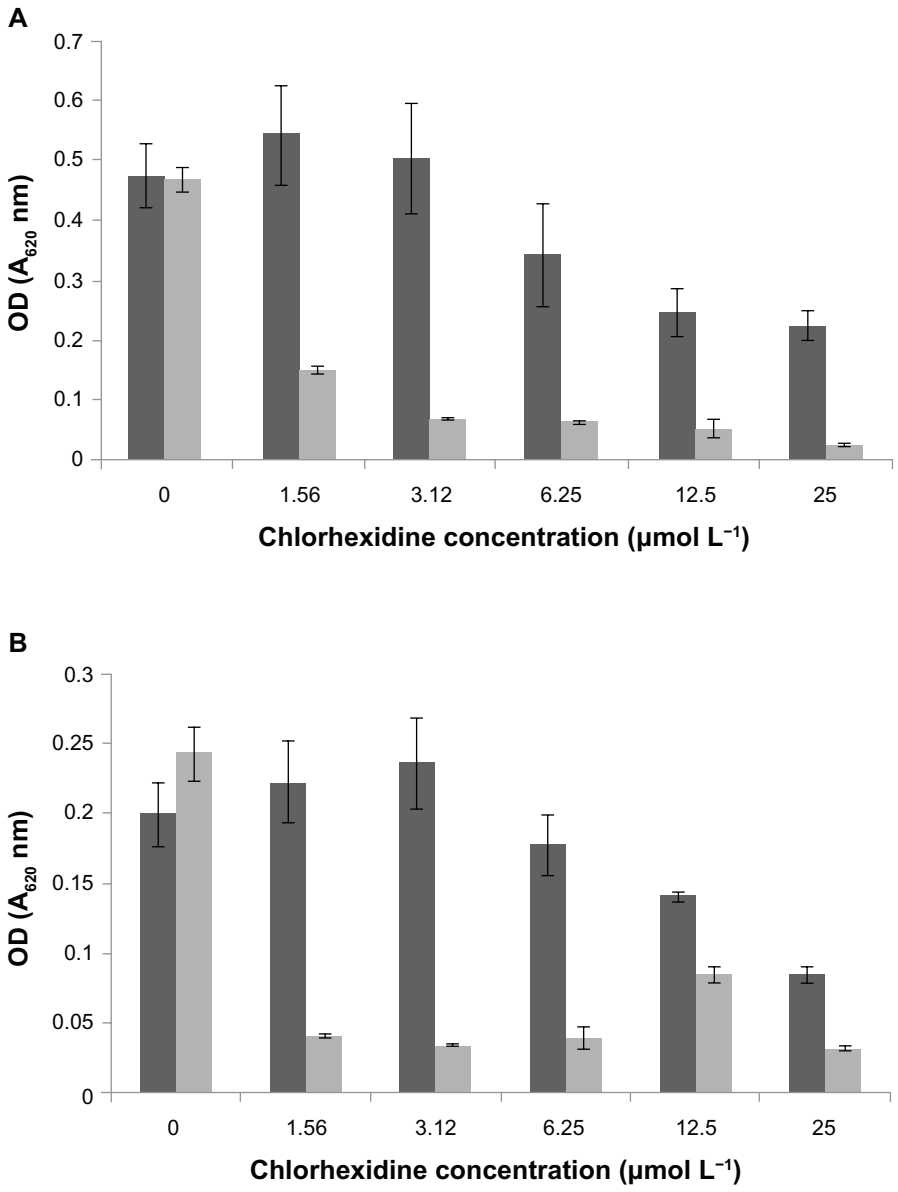

Figure 10 Minimum inhibitory concentrations of CHX and CHX-HMP-5 against (**A**) MRSA and (**B**) *Pseudomonas aeruginosa*.
Notes: The dark grey bars represent 25 μmol L^{-1} CHX; the light grey bars represent CHX-HMP-5. Absorbance at 620 nm.
Abbreviations: CHX, chlorhexidine; CHX-HMP-5, chlorhexidine hexametaphosphate (5 mmol L^{-1}); MRSA, methicillin-resistant *Staphylococcus aureus*; OD, optical density.

solution bathing the colloid. Furthermore, the biofilm studies indicated that the CHX-HMP-5 colloid was efficacious against biofilms of MRSA and *P. aeruginosa* in vitro. The next step in evaluating the antimicrobial and antibiofilm efficacy of the CHX-HMP NPs will be to establish how many bacteria on the differently functionalized surfaces are metabolically active, by using a live/dead staining technique.

Both MRSA and *P. aeruginosa* are nosocomial pathogens that can easily be introduced into wounds, for example postsurgery. They may be found on fomites and surfaces in health care settings and are transferred to wounds as a consequence of poor hygienic practice. MRSA is resistant to numerous antibiotics, making it very difficult to treat, and *P. aeruginosa* is intrinsically resistant to antibacterial treatment, meaning it is problematic to eradicate. Both organisms will readily colonize a wound site or the surface of an implant, where they can grow as part of a mixed-biofilm; biofilm bacteria exhibit increased tolerance to antimicrobial treatments. Prior to colonization and the development of a biofilm, microorganisms exist in the planktonic form, which is generally more susceptible to antimicrobial treatment. The fact that CHX-HMP-5 was efficacious against both bacterial lifestyles suggests it could be a good preventer of colonization, as well as an effective treatment.

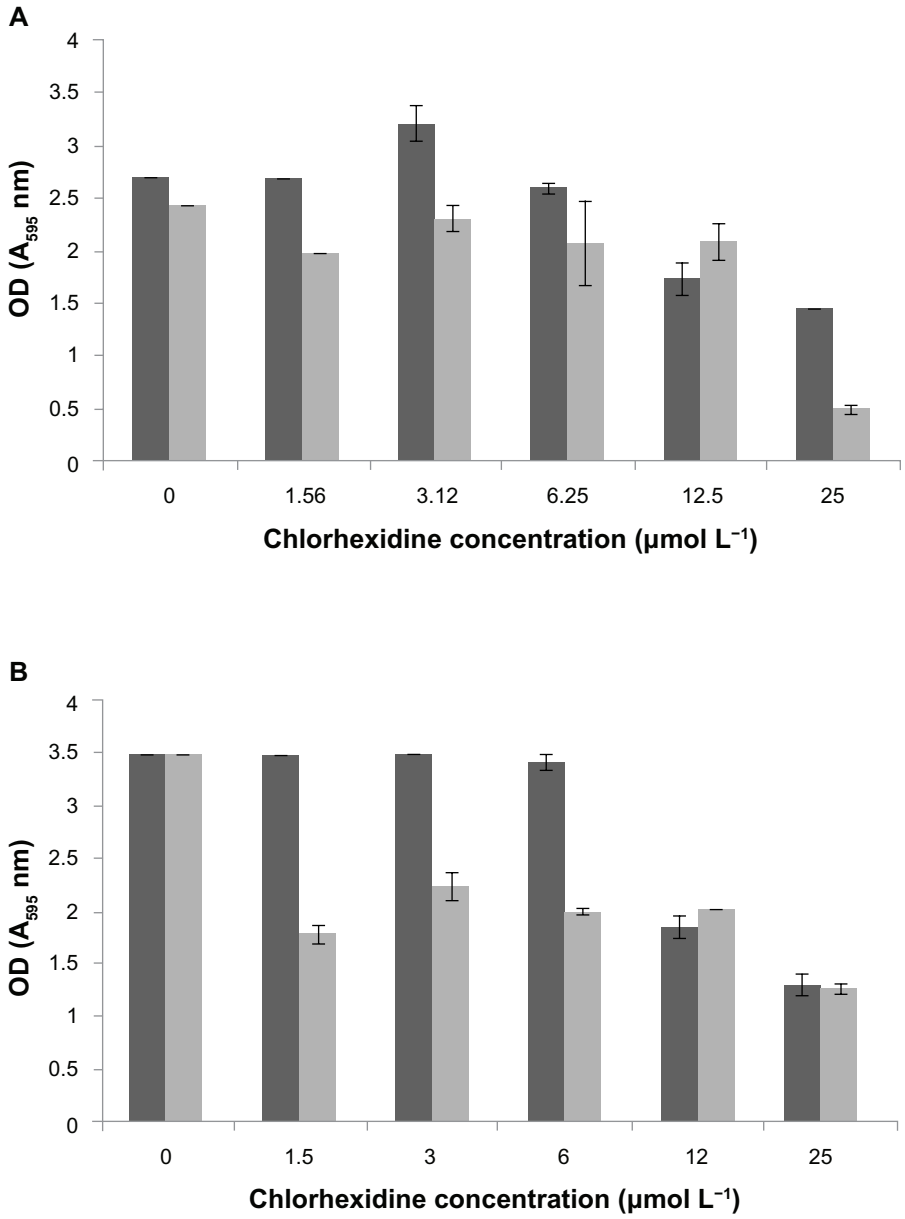

Figure 11 Biofilm disruption following treatment with CHX or CHX-HMP-5 against (**A**) MRSA and (**B**) *Pseudomonas aeruginosa.*
Notes: The dark grey bars represent 25 μmol L^{-1} CHX; the light grey bars represent CHX-HMP-5. Absorbance at 595 nm.
Abbreviations: CHX, chlorhexidine; CHX-HMP-5, chlorhexidine hexametaphosphate (5 mmol L^{-1}); MRSA, methicillin-resistant *Staphylococcus aureus*; OD, optical density.

Conclusion

The CHX-HMP NPs described here formed a stable colloid with particle size over the range ~20–160 nm and a zeta potential of ~—50 mV. The colloids lend themselves to the dip coating of several material types, including metal oxide, glass, and an elastomeric wound dressing, all of which were coated in deposits of porous NP aggregate. Each material displayed an extended release of soluble CHX following CHX-HMP NP-functionalization, which was sustained for at least 50 days. The NP colloid exhibited antimicrobial efficacy against MRSA and *P. aeruginosa*, in both planktonic and biofilm growth conditions. These antimicrobial NPs may find application in a range of biomedical materials and consumer products.

Acknowledgments

The authors are grateful to Dr Neil Fox for carrying out the vacuum deposition of the titanium and Dr David Williams for his expertise with the DLS. NJW is funded by an EPSRC (Engineering and Physical Sciences Research Council) PhD studentship.

Disclosure

The authors report no conflicts of interest in this work.

References

1. McDonnell G, Russell AD. Antiseptics and disinfectants: activity, action, and resistance. *Clin Microbiol Rev*. 1999;12(1):147–179.
2. Meyer B, Cookson B. Does microbial resistance or adaptation to biocides create a hazard in infection prevention and control? *J Hosp Infect*. 2010;76(3):200–205.
3. Milstone AM, Passaretti CL, Perl TM. Chlorhexidine: expanding the armamentarium for infection control and prevention. *Clin Infect Dis*. 2008;46(2):274–281.
4. Barbour ME, Gandhi N, el-Turki A, O'Sullivan DJ, Jagger DC. Differential adhesion of Streptococcus gordonii to anatase and rutile titanium dioxide surfaces with and without functionalization with chlorhexidine. *J Biomed Mater Res A*. 2009;90(4):993–998.
5. Raad I, Mohamed JA, Reitzel RA, et al. Improved antibiotic-impregnated catheters with extended-spectrum activity against resistant bacteria and fungi. *Antimicrob Agents Chemother*. 2012;56(2):935–941.
6. Verraedt E, Pendela M, Adams E, Hoogmartens J, Martens JA. Controlled release of chlorhexidine from amorphous microporous silica. *J Control Release*. 2010;142(1):47–52.
7. Cheng L, Weir MD, Xu HH, et al. Antibacterial and physical properties of calcium-phosphate and calcium-fluoride nanocomposites with chlorhexidine. *Dent Mater*. 2012;28(5):573–583.
8. Fong N, Poole-Warren LA, Simmons A. Development of sustained-release antibacterial urinary biomaterials through using an antimicrobial as an organic modifier in polyurethane nanocomposites. *J Biomed Mater Res Part B Appl Biomater*. 2013;101(2):310–319.
9. Barbour ME, O'Sullivan DJ, Jagger DC. Chlorhexidine adsorption to anatase and rutile titanium dioxide. *Colloid Surface A: Physiochemical and Engineering Aspects*. 2007;307(1–3):116–120.
10. BSAC. *BSAC Methods for Antimicrobial Susceptibility Testing*. Version 11.1. Birmingham: British Society for Antimicrobial Chemotherapy; 2012. Available from: http://bsac.org.uk/wp-content/uploads/2012/02/Version-11.1-2012-Final-.pdf. Accessed August 8, 2013.
11. Miles AA, Misra SS, Irwin JO. The estimation of the bactericidal power of the blood. *J Hyg (Lond)*. 1938;38(6):732–749.
12. Hanaor D, Michelazzi M, Leonelli C, Sorrell CC. The effects of carboxylic acids on the aqueous dispersion and electrophoretic deposition of ZrO2. *J Eur Ceram Soc*. 2012;32(1):235–244.
13. Gottrup F, Apelqvist J, Price P; European Wound Management Association Patient Outcome Group. Outcomes in controlled and comparative studies on non-healing wounds: recommendations to improve the quality of evidence in wound management. *J Wound Care*. 2010;19(6):237–268.
14. James GA, Swogger E, Wolcott R, et al. Biofilms in chronic wounds. *Wound Repair Regen*. 2008;16(1):37–44.
15. Ammons MC. Anti-biofilm strategies and the need for innovations in wound care. *Recent Pat Antiinfect Drug Discov*. 2010;5(1):10–17.
16. Storm-Versloot MN, Vos CG, Ubbink DT, Vermeulen H. Topical silver for preventing wound infection. *Cochrane Database Syst Rev*. 2010CD006478.
17. Sofokleous P, Stride E, Edirisinghe M. Preparation, characterization, and release of amoxicillin from electrospun fibrous wound dressing patches. *Pharm Res*. 2013;30(7):1926–1938.
18. Eardley WG, Watts SA, Clasper JC. Limb wounding and antisepsis: iodine and chlorhexidine in the early management of extremity injury. *Int J Low Extrem Wounds*. 2012;11(3):213–223.
19. Wu SC, Crews RT, Zelen C, Wrobel JS, Armstrong DG. Use of chlorhexidine-impregnated patch at pin site to reduce local morbidity: the ChIPPS Pilot Trial. *Int Wound J*. 2008;5(3):416–422.
20. Agarwal A, Nelson TB, Kierski PR, et al. Polymeric multilayers that localize the release of chlorhexidine from biologic wound dressings. *Biomaterials*. 2012;33(28):6783–6792.
21. Türkün LS, Türkün M, Ertuğrul F, Ateş M, Brugger S. Long-term antibacterial effects and physical properties of a chlorhexidine-containing glass ionomer cement. *J Esthet Restor Dent*. 2008;20(1):29–44.
22. Hu G, Xiao L, Tong P, et al. Antibacterial hemostatic dressings with nanoporous bioglass containing silver. *Int J Nanomedicine*. 2012;7:2613–2620.
23. Renoud P, Toury B, Benayoun S, Attik G, Grosgogeat B. Functionalization of titanium with chitosan via silanation: evaluation of biological and mechanical performances. *PLoS ONE*. 2012;7(7):e39367.
24. Hickok NJ, Shapiro IM. Immobilized antibiotics to prevent orthopaedic implant infections. *Adv Drug Deliv Rev*. 2012;64(12):1165–1176.

International Journal of Nanomedicine

Dovepress

Publish your work in this journal

The International Journal of Nanomedicine is an international, peer-reviewed journal focusing on the application of nanotechnology in diagnostics, therapeutics, and drug delivery systems throughout the biomedical field. This journal is indexed on PubMed Central, MedLine, CAS, SciSearch®, Current Contents®/Clinical Medicine, Journal Citation Reports/Science Edition, EMBase, Scopus and the Elsevier Bibliographic databases. The manuscript management system is completely online and includes a very quick and fair peer-review system, which is all easy to use. Visit http://www.dovepress.com/testimonials.php to read real quotes from published authors.

Submit your manuscript here: http://www.dovepress.com/international-journal-of-nanomedicine-journal